

# Optimization of optical uniformity factors of backlight module using robust design method

JU-CHI WANG<sup>1</sup>, YU-CHENG FAN<sup>1</sup>, TE-HUA FANG<sup>1\*</sup>, ANH-SON TRAN<sup>1,2</sup>, YU-TING CHENG<sup>1</sup>

<sup>1</sup>Department of Mechanical Engineering,  
National Kaohsiung University of Science and Technology,  
Kaohsiung 80778, Taiwan

<sup>2</sup>Faculty of Mechanical Engineering,  
Hung Yen University of Technology and Education,  
Khoai Chau District, Hung Yen Province, Vietnam

\*Corresponding author: fang.tehua@msa.hinet.net

In order to meet the advent of the high-definition liquid crystal display (LCD) era, in addition to the high-quality panel manufacturing technology, how the backlight module can provide a uniform backlight with higher uniformity for a better experience in viewing, is a very important and urgent issue. In this study, the 15.6-inch side-in backlight module was used as the benchmark, and the Taguchi method was applied to find the high uniformity. The matching of the fishbone diagram affects the optical uniformity factor of the backlight module, such as the size of the light guide plate dot, the color of the plastic frame, the color of the fixed gel of the light guide plate, and the difference of the reflection surface. The optical analog software LightTools is used according to the orthogonal table. The signal-to-noise (S/N) ratio of the average uniformity characteristics is obtained, then it is converted into the best response factor of the factor response table and the factor reaction diagram. The homogeneity at 13 points is as high as 90.12%, which is 4.72% higher than the original design factor. The contribution of the four factors to the uniformity can be obtained by using the variance analysis. Finally, the influence of each factor level on the uniformity is discussed.

Keywords: backlight module, uniformity, Taguchi method, LightTools.

## 1. Introduction

The backlight module is one of the key components of the liquid crystal display. The structure of the liquid crystal display is composed of a liquid crystal panel and a backlight module [1]. The “liquid crystal” in the liquid crystal panel itself is a chemical material having no light-emitting characteristics, so the liquid crystal panel needs a backlight to support the image, and the backlight is “Backlight Module” which is shown in Fig. 1. It is mainly composed of five major parts, including iron parts, plastic frames, diaphragms, light sources, light guide plates or diffusers. In the design of the

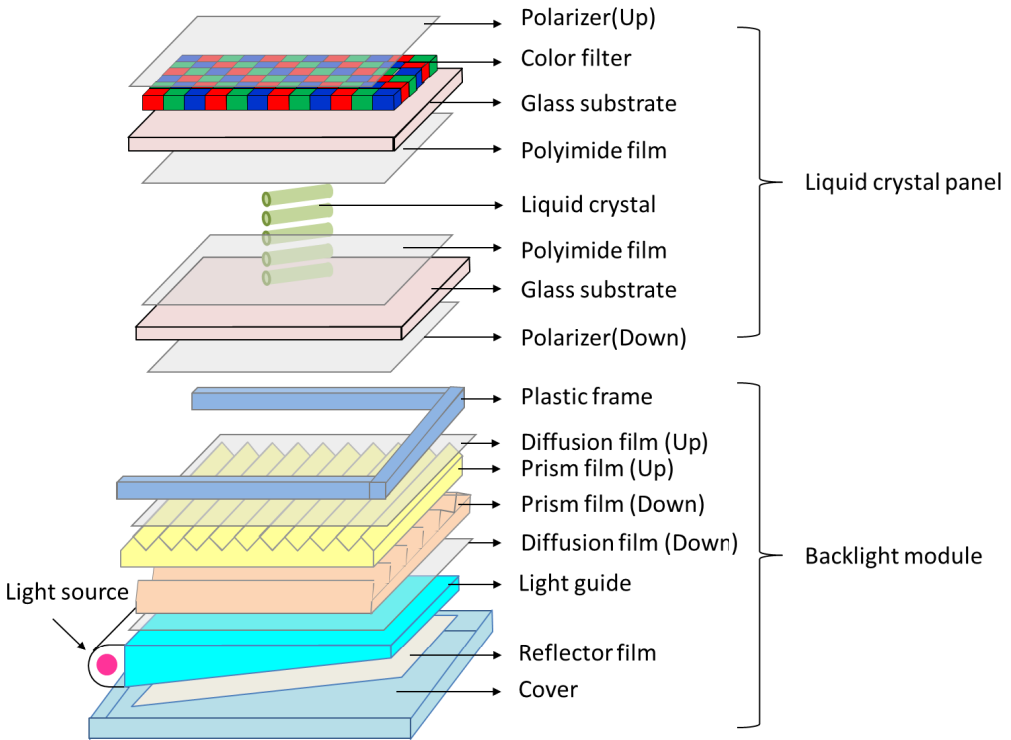


Fig. 1. A schematic diagram of a liquid crystal display (LCD).

backlight module, different color temperatures and uniform light sources can be provided for the liquid crystal panel. According to the source position of the light source, the design categories can be divided into two categories: a “direct type backlight module” and a “side-in backlight module”.

In 2007, CHANG *et al.* [2] used a molecular dynamics (MD) to obtain a high uniformity in the design of the light guide plate using a variable regional dot density ratio. Under the initial backlight module, an equal dot density design was used to confirm the energy direction of the light source. The end energy of the group is reduced, the dot density ratio is increased, and the energy of the end light source can be pulled up. On the 1.8-inch and 15-inch backlight modules, a high uniformity of more than 90% can be obtained. LIN *et al.* [3] carried out the best experimental design of the color mixing zone of the Taguchi method. Among them, the micro-structure shape, angle, size and light guide plate type of the light guide plate were listed as the control factors, and each of them had three levels of  $L_9$  orthogonal table experimental design. The slope of the wedge-shaped light guide is designed to have a slope of  $0.3^\circ$  via the S/N conversion optimum factor combination, and a prism glass-type microstructure is used, which has a design size of 0.2 mm and an angle of  $44^\circ$ . An 85% homogeneity can be obtained in optical performance. JOO *et al.* [4] used the dot density distribution to optimize the light guide

plate under the analysis of optical simulation software LightTools. It was found that under the limitation of the small size of the backlight module, the design of the direct-type and side-entry backlight modules was 85.6% and 94.28%, the difference is 8.68%, indicating that the small-size backlight module is more suitable for the side-in design, and can obtain higher uniformity. The robust design method, also called the Taguchi method, has been used successfully in many industrial applications of fabrication, component design and optimization [5–7].

In this study, the 15.6-inch side-in backlight module was used as the benchmark, and the Taguchi method was applied to find the high uniformity. The design of the backlight module uses fishbone diagrams to select the control factors for analysis, which are the dot size, the color of the plastic frame, the color of the fixed glue, and the reflector surface of the light guide plate. It is expected that the future development of the backlight module can be used to design this factor. A higher uniformity creates a higher quality LCD display.

## 2. Methods

### 2.1. Taguchi methods

The Taguchi method is based on the use of experimental planning and statistical techniques, using the design of the orthogonal table and the analysis of the variance, so that the trial production stage can reduce the number of experiments and improve the experimental data analysis method under the condition of maintaining reliability, and the impact of the interference factor [8, 9]. It minimizes and identifies the factors that reduce process and quality variation to achieve optimal process design parameters. The quality of a product can be explained by many factors, and these factors are called quality characteristics. The unit of measurement of the quality characteristics refers to the signal-to-noise ratio (S/N ratio) to determine whether the target has been achieved and used  $\eta$  represents the unit in decibels (dB). When the S/N ratio is larger, the overall quality loss is smaller, and *vice versa*. The desired goals according to quality characteristics can be divided into three categories: nominal the best (NTB), smaller the best (STB), and larger the best (LTB). Experimental design is a set of experiments that introduce changes related to experimental results through the introduction of a variable. Such a variable is called a factor. The factors affecting quality characteristics in the Taguchi method can be divided into signal factors, control factors and noise factors.

A table of Taguchi orthogonal arrays is an experimental configuration table of factors and level numbers using partial factor experiments in the full factor experiment. The purpose is to obtain an estimate of the effect of the reliability factor using fewer experiments [10]. This study is straight through the Taguchi type. The table is matched with the S/N ratio of the large characteristics to obtain the estimated value of the control factor affecting the quality characteristics effect, and the orthogonal table is described by  $L_a(b^c)$ ,  $L$  is the orthogonal table, and there are  $a$  group of experiments, which can accommodate up to  $b$  kinds. There are  $c$  number of factors and the number of factors.

## 2.2. Optical simulation software

LightTools optical simulation software features optical precision interactive 3D solid modeling that directly describes light sources, lenses, mirrors, diffractive optics, cymbals, mechanical structures, and optical paths in optical systems, and precisely defines the shape of the actual light source and features [11]. Monte Carlo method ray tracing can be realized by using the illumination module to determine the illuminance, intensity and brightness on the specified surface, and in system modeling, it can be directly on the 2D, 3D wireframe or 3D solid image [12]. Through various operations, the shape of the component can be realized by basic solid modeling Boolean operations (join, intersection, difference set) to realize complex geometry, and ray tracing function, and the optical simulation results are quantized into numerical values. The optical homogenization factor parameter simulation requirements were used by the optical simulation software LightTools as parameters of the optical simulation quantization factor.

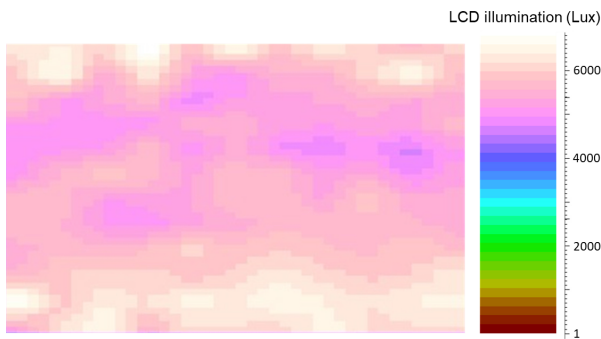


Fig. 2. Numerical simulation in the luminous surface.

Grid data is the main way of optical analog software LightTools optical analog data representation. The general data is mostly composed of 9, 13, 121 points, *etc.*, and the number of cutting grids can be increased according to user requirements. The data analysis, such as the trend of light source changes or the simulation of the light-emitting surface of the backlight module, is shown in Fig. 2.

## 2.3. Optical basic theory of backlight module

The optical principle of the backlight module is based on the principle of geometric optics, which discusses the law of linear propagation of light, indicating that the light source will refract and reflect when it enters different media.

Uniformity is a measure of the change in optical brightness on the surface of a display. If the uniformity is 100%, the brightness is completely uniform across the surface of the display as follows [13]:

$$\text{Uniformity} = \frac{L_{\min}}{L_{\max}} \times 100\%$$

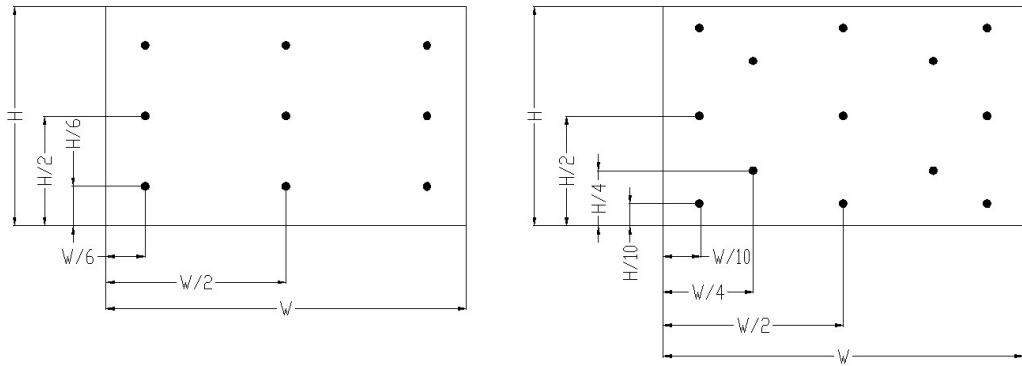


Fig. 3. Common measurement points.

The ratio of the maximum value of the measured luminance to the minimum luminance is calculated. The quantized result is represented by percentage (%). The commonly used measurement point is the 9-point measurement point or the 13-point measurement point, as shown in Fig. 3.

The optical trend is to discuss the distribution of light source energy from the beginning to the end on the light guide plate. The measured value is the luminance ( $\text{cd}/\text{m}^2$ ), the energy of the optical trend source is changed, the surface structure of the light guide plate is adjusted, and the light source is guided to achieve the target distribution. When discussing the optical trend, the industry will divide the length and width of the light guide into 11 points. The long dimension is defined as the  $x$ -axis and the wide dimension is defined as the  $y$ -axis.  $P(x)$ -1- $P(x)$ -11 points and  $P(y)$ -1- $P(y)$ -11 points, and in the long-size  $P(x)$ -6 points, due to sorting at the center of the long 11-point position, the phase corresponding  $P(y)$ -1- $P(y)$ -11 points can also be called “optical central trend”, and because the central trend of optics is located in the center of the light guide plate, it is less affected by external factor variation, so it is often used to represent the whole. Optical trends are shown in Fig. 4.

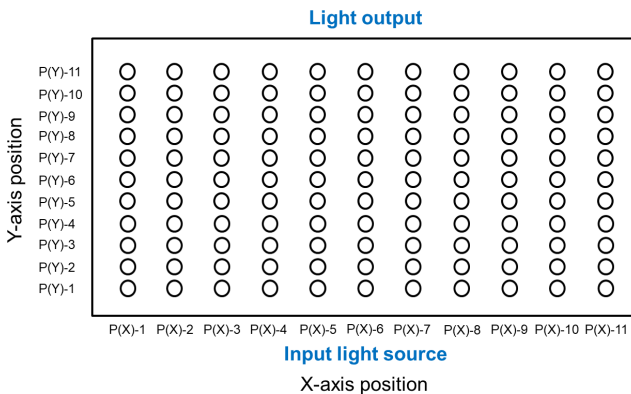


Fig. 4. Optical characteristics of the light guide plate explains the cast from a light source.

### 3. Results and discussion

#### 3.1. Factors affecting evaluation influence in the uniformity of backlight modules

Before choosing the factors that affect the uniformity of the backlight module, it is necessary to understand how the variation of the uniformity is generated, in order to understand the influence of the factors on the uniformity. A backlight module had to be designed at the expansion-contraction effect, due to the difference in thickness of the enamel film, a phenomenon of warpage occurs during the startup of the light source, which affects the measurement data of the CCD thermal imager machine. Comparing 0.3 and 1.2 mm at the expansion-contraction on the  $x$ -axis, the uniformity is 7% difference [14]. When the surface structure of the prism is designed as a triangular matrix, the uniformity adjusts the structure and density of the prism in different regions, which has a 12% difference with the trend of the surface light source [15]. If compared with the reflective sheet, it can be found that when the reflective sheet is removed, the surface light source is uneven in brightness, resulting in a 6% overall reduction in uniformity [16]. In this study, the optical simulation software LightTools is used to simulate the requirements of the optical homogeneity factor parameters, and the light source database in the software and the built-in preset materials are used for selection. The surface characteristics of the materials can be adjusted according to the reflection characteristics of the actual parts. Set to avoid errors caused by warped light sources.

#### 3.2. Control factors of the uniformity

Previous studies have investigated the factors that changed the dot shape, dot depth, dot density, diffuser, and reflector of the light guide plate, *i.e.* the influence factors of the uniformity [17–21]. However, the study is lacking with colors of the plastic frame and fixing stuff. The design of the backlight module uses fishbone diagrams to select the control factors for analysis, which are the dot size, the color of the plastic frame, the color of the fixed glue, and the reflector surface of the light guide plate. Each factor has three levels, and its control factors are shown in Table 1. Taguchi  $L_9(3^4)$  orthogonal array with four experimental parameters is shown in Table 2.

Table 1. Controllable factors under various types.

Factor	Control factors	Level 1	Level 2	Level 3
<i>A</i>	The size of dot pattern distribution located on light guide plates	0.023 mm	0.025 mm	0.027 mm
<i>B</i>	The color of plastic frame	Gray	White	Black
<i>C</i>	The color of adhesive tapes	Transparent	White	Black
<i>D</i>	Types of reflective surfaces	Specular	Semi-specular	Matte

T a b l e 2. The experimental design used orthogonal array  $L_9(3^4)$  to demonstrate the various types of controllable factors. Uniformity parameters used the ANSI (American National Standards Institute) 13-point illumination uniformity to simulate S/N ratio.

Experiment number	Levels and factors				The ANSI 13-point illumination uniformity [%]				$\eta_{LBT}$ [dB]
	<i>A</i>	<i>B</i>	<i>C</i>	<i>D</i>	15 min	30 min	45 min	60 min	
1	1	1	1	1	85.53	85.47	85.5	85.56	37.76
2	1	2	2	2	76.02	76.10	76.08	76.06	37.52
3	1	3	3	3	77.5	77.53	77.55	77.49	37.56
4	2	1	2	3	80.09	80.13	80.14	80.15	38.29
5	2	2	3	1	77.24	77.15	77.08	77.17	37.16
6	2	3	1	2	73.95	73.99	74.02	74.00	37.25
7	3	1	3	2	65.12	65.09	65.07	65.05	37.73
8	3	2	1	3	75.96	75.91	75.93	75.98	38.16
9	3	3	2	1	73.16	73.19	73.16	73.25	36.67

**3.3. Influence factor of the uniformity discussed by quality characteristics analysis**

There are totally 9 experiments to be simulated and each experiment is based on an  $L_9$  orthogonal array using LightTools as presented in Table 2. The simulation time is set at variance 15, 30, 45, and 60 minutes, respectively. In this study, the performance statistics is achieved by using “the larger the better” to define the optimum conditions. Uniformity parameters used the American National Standards Institute (ANSI) 13-point illumination uniformity to simulate S/N ratio as shown in Table 2.

**3.4. Influence factor of the uniformity for analysis of variance (ANOVA)**

In order to analyze the influence of each control factor on the experimental results, use the variance analysis (Table 3) to calculate the contribution of each control factor, and obtain the square sum of *A* factor  $SS_A = 0.01290$ , the contribution is 0.64%; the sum of the square of *B* factor  $SS_B = 0.89226$ , the contribution degree is 44.57%; the sum of the squares of the *C* factor  $SS_C = 0.11083$ , the contribution degree is 5.54%; the

T a b l e 3. Variation analysis table.

Factor	SS	DOF	Var	Contribution [%]
<i>A</i>	0.0129	2	0.00645	0.64
<i>B</i>	0.89226	2	0.44613	44.57
<i>C</i>	0.11083	2	0.05542	5.54
<i>D</i>	0.98612	2	0.49306	49.25
Total	2.0021	8	–	100

sum of the squares of the  $D$  factor  $SS_D = 0.98612$ , the contribution degree is 49.25%, and the factor contribution rank is  $D$  factor  $>$   $B$  factor  $>$   $C$  factor  $>$   $A$  factor.

### 3.5. The parameters optimization for computational lighting uniformity simulation

Obtain the best factor combination as  $A_1B_1C_1D_3$  through the  $\eta_{U-LTB}$  factor response table and  $\eta_{U-LTB}$  factor response diagram (Fig. 5), and the original design factor is  $A_2B_2C_1D_3$ ; import the original design factor and the best factor into the optical simulation software LightTools. The simulation conditions are the total energy of a fixed light source and the number of rays of light 10 million, the simulation time is 60 minutes, the simulation results obtained for the original design factor with 13 points the optical simulation uniformity is 85.40%, the best factor with 13 points the optical simulation uniformity is 90.12%. After comparison, it can be seen that the homogeneity of the best factor collocation is improved by 4.72% compared with the homogeneity of the original design factor.

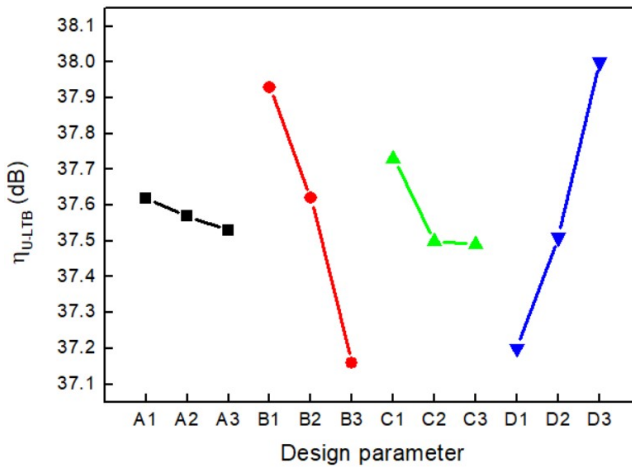


Fig. 5. Interaction plots for controllable factors, in order to find the optimal levels of the four process parameters.

### 3.6. Impact analysis of controllable factors

Under the condition that the total energy of the light source is fixed, based on the original design factor  $A_2B_2C_1D_3$ , select a factor and change its factor level one by one, while the other control factor levels remain unchanged, perform optical simulation of the selected factor at different levels. Compare the results, taking factor  $A$  as an example, change the level of factor  $A$ , while the level of other control factors remain unchanged, namely  $A_1B_2C_1D_3$ ,  $A_2B_2C_1D_3$ ,  $A_3B_2C_1D_3$ , and compare the optical simulation results of the three levels of factor  $A$ , and so on. Respectively, one can get four sets of factor analysis.



**3.6.1. Factor A: analysis of the difference in dot size of the light guide plate**

The combination of the three level variations of the factor  $A$  is used to analyze the central trend data of the optical simulation. Based on the original design factor  $A_2$ , the optical trend of the  $A_2$  level is compared with the other two levels. From the difference of the optical trends at each point, the total energy of the three levels is the same. The energy of the light source changes with the size of the dot. The minimum dot of the  $A_1$  level light guide plate is 0.023 mm, which will bring the energy of the light source to the output end, resulting in a lower light source energy on the incident side. 0.025 mm between the  $A_1$  and  $A_3$  levels, will move partly the light source energy at the light entrance

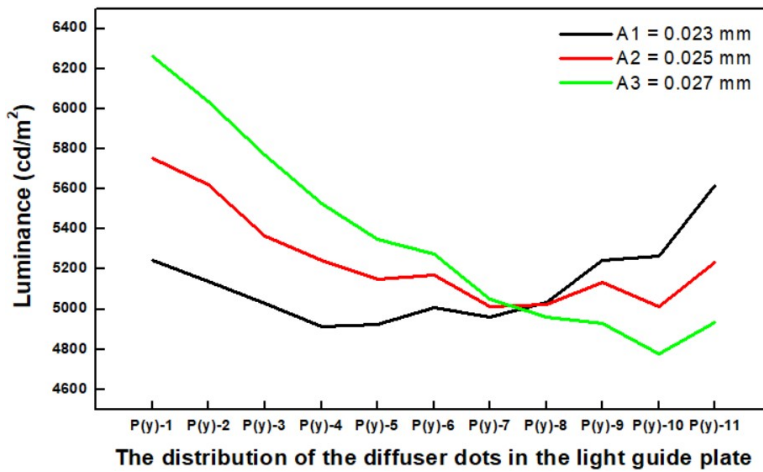


Fig. 6. The luminance in the simulation results were shown the size of dot pattern distribution located on light guide plates.

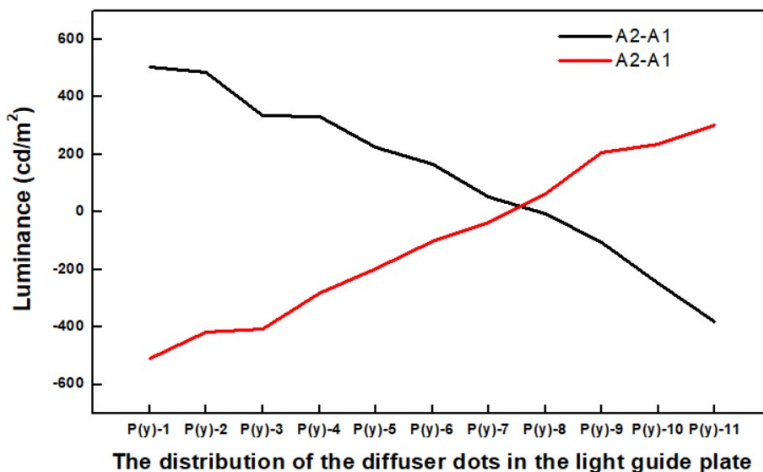


Fig. 7. The luminance distribution of the controllable factors in the simulation results were shown the size of dot pattern distribution located on light guide plates.

side to the light output end, resulting in a slight decrease in the light source energy at the light entrance side and a slight increase in the light energy at the light end. The maximum dot size is 0.027 mm, and the energy of the light source will stay on the light-entering side, resulting in a lower energy condition of the light source at the light output end, as shown in Figs. 6 and 7. The larger the dot, the easier the energy of the light source stays on the light-entering side; the smaller the dot, the easier the energy of the light source is taken to the output end.

### 3.6.2. Factor *B*: color difference analysis of plastic frame

The combination of the three level variation of the *B* factor is used to analyze the central trend data of the optical simulation. Based on the original design factor  $B_2$ , the  $B_2$  level is compared with the other two levels for the optical central trend. From the difference between the optical trends of each point, the three levels are the same. Under the energy, we can see that there are the three levels under the same total energy of the light source, the energy loss of the light source is ranked as  $B_3$  level >  $B_2$  level >  $B_1$  level. The  $B_1$  level is a white plastic frame. White can reflect the light source, so the energy of the light source at the light end will be reflected back. The energy at the light source is higher and the overall energy loss of the light source is lower when the light board is used;  $B_2$  level is gray plastic frame, the color is dark series, but not all black, so it retains the characteristics of absorbing energy and reflecting light energy. So, only part of the light source energy at the light exit end can be reflected back to the light guide plate. The  $B_3$  level is a black plastic frame, black absorbs the light source energy, resulting in a decrease in the overall optical analog brightness. The closer the light exit end is, the greater the energy range of the light source as displayed in Figs. 8 and 9. The energy of the point light source at the end of the white plastic frame is higher; the energy of the point light source at the end of the gray plastic frame or black plastic frame will be lower, and the optical analog brightness of the black plastic frame on P(y)-9 will sud-

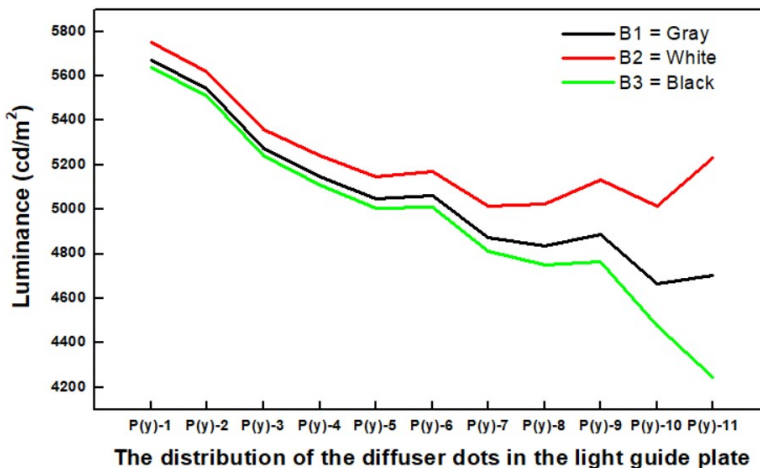


Fig. 8. The luminance on the white plastic frame in simulation results.

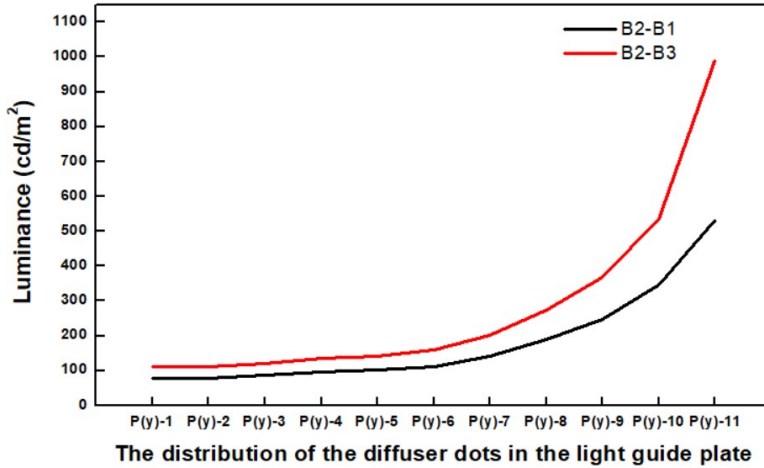


Fig. 9. The luminance distribution of the controllable factors in the simulation results were shown the color of plastic frame on light guide plates.

denly drop to P(y)-11, the overall light source energy of both is less than the white plastic frame.

**3.6.3. Factor C: color difference analysis of light guide plate fixing colloid**

The combination of the three level variation of the C factor is used to analyze the central trend data of the optical simulation. Based on the original design factor C<sub>1</sub>, the C<sub>1</sub> level is compared with the other two levels for the optical central trend. From the difference of the optical trend at each point, we can know that the three levels are at the same light source. Under the total energy, the energy loss of the light source is ranked as C<sub>3</sub> level > C<sub>1</sub> level > C<sub>2</sub> level. C<sub>1</sub> level is the transparent light guide plate fixing glue.

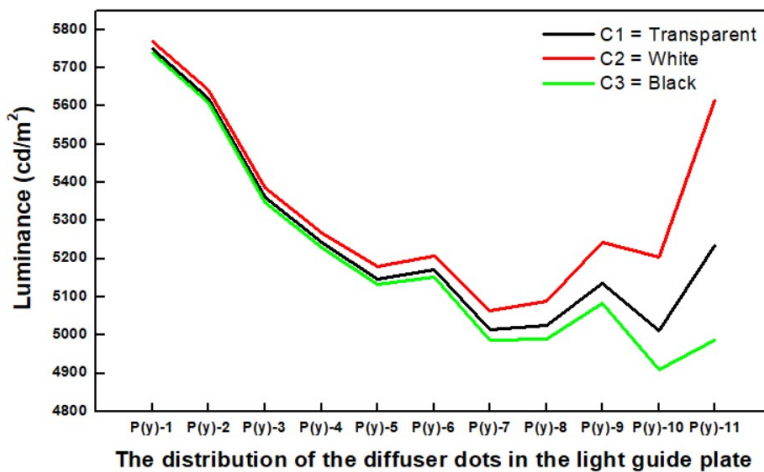


Fig. 10. The luminance in the simulation results were offering colored adhesive tapes on light guide plates.

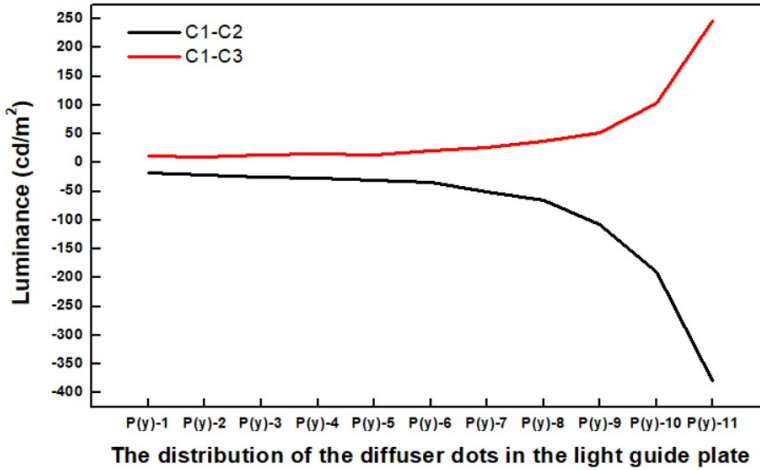


Fig. 11. The luminance distribution of the controllable factors in the simulation results were shown the colored adhesive tapes on light guide plates.

The transparent colloid has the effect of condensing the light source, which can maintain the energy of the light source at the same level or slightly increased  $C_2$ . The  $C_2$  level is white light guide plate fixing glue. The white can reflect the light source, so the energy at the light source will be reflected back into the light guide plate, resulting in the energy at the light source is higher and the overall energy loss of the light source is lower.  $C_3$  level is black light guide plate fixed glue and black will absorb the energy of the light source, resulting in a decrease in the overall optical analog brightness. The closer to the light output end, the greater the amplitude of the light source energy absorbed, as shown in Figs. 10 and 11. The transparent light guide plate fixing glue can maintain the end light source energy at the same level or slightly increased; the white light guide plate fixing glue can obviously improve the end light source energy; the black light guide plate fixing glue will cause the end point light source energy to be lower.

### 3.6.4. Factor $D$ : analysis of the surface difference of the reflector

The combination of the three variation level of the factors  $D$  is used to analyze the central trend data of the optical simulation. Based on the original design factor  $D_3$ , the  $D_3$  level is compared with the other two levels for the optical central trend. From the difference between the optical trends of each point, we can know that the three levels are at the same light source. Under the total energy, the energy loss of the light source is ranked as  $D_3$  level  $>$   $D_2$  level  $>$   $D_1$  level.  $D_1$  level is a mirror-type reflector. Its reflective surface is generally smooth like a mirror, which is more in line with the mirror reflection phenomenon in the reflection law, so the energy of the light source is higher. There is no loss, and its reflection characteristics bring the energy of the light source at the light end to the light side.  $D_2$  level is a mirror-type matte reflector, its reflective surface is not completely smooth, and the reflection characteristics of the light source have specular reflection and diffusion phenomena. Therefore, the energy of the light

source will be slightly lost, and its reflection characteristics have the phenomenon that the energy of the light source on the light entrance side is higher, and the energy of the light source on the light output side is lower. The diffuse phenomenon in the law of reflection has a reflection characteristics that the light will be reflected irregularly in different directions, thus causing more energy loss from the light source, as shown in Figs. 12 and 13.

The reflection characteristics of the light source of the specular reflection sheet are more in line with the ideal specular reflection phenomenon, so that the energy of the light source is less lost during the energy reflection process, and the energy of the light

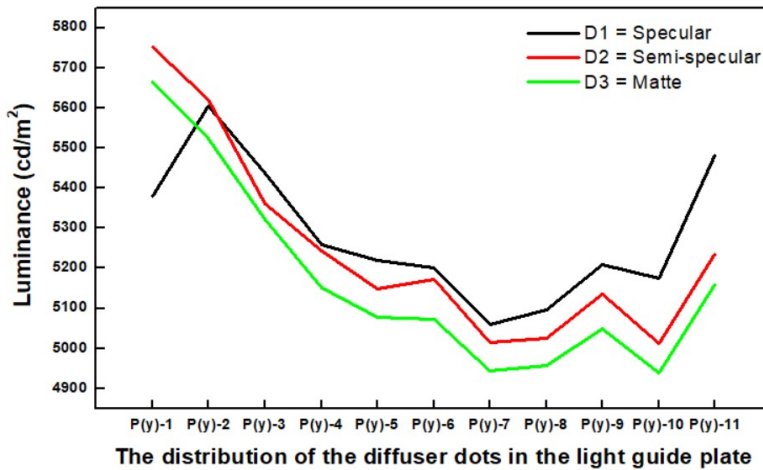


Fig. 12. The luminance in the simulation results were offering specular, semi-specular, and matte reflector film on light guide plates, respectively.

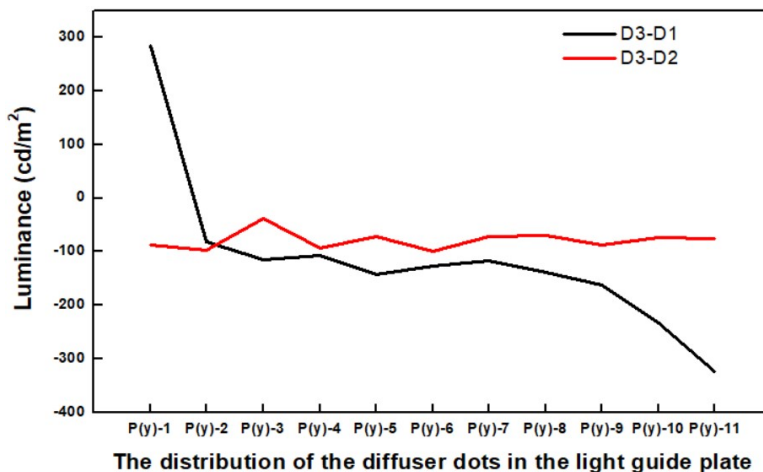


Fig. 13. The luminance distribution of the controllable factors in the simulation results were offering specular, sputter, and matte reflector film on light guide plates, respectively.

source on the light input side is moved to the output end; the reflection characteristics of the light source of the specular reflection sheet has a mirror surface The reflection and diffusion phenomena make the light source on the incident side have higher energy and the end light source has lower energy; the reflection characteristics of the general matte reflector are more in line with the ideal diffuse reflection phenomenon, so the overall light source energy will be more reflective than the mirror type matte The film is low, but the trend is similar.

## 4. Conclusions

In summary, it is known that as long as the uniform surface light source is affected, the homogeneity will be affected. In this study, we select the control factors for analysis, which are the dot size, the color of the plastic frame, the color of the fixed glue, and the reflector surface of the light guide plate for comparison between the homogeneity and the heterogeneity of the uniformity.

1) According to the  $\eta_{U-LTB}$  factor response results, the best factor combination is  $A_1B_1C_1D_3$ , that is, the dot size of the  $A_1$  light guide plate is 0.023 mm, the S/N ratio = 37.62 dB, the  $B_1$  gray plastic frame, the S/N ratio = 37.93 dB, the  $C_1$  transparent light guide plate Fixed colloid, S/N ratio = 37.73 dB,  $D_3$  = general matte reflector, S/N ratio = 38.0 dB; 13-point optical simulation uniformity and original design factor  $A_2B_2C_1D_3$  increased by 4.72%, gain 1.055 times.

2) The contribution of each control factor in this study is the dot size of the factor  $A$  light guide plate dot 0.64%, the factor  $B$  plastic frame color 44.57%, the factor  $C$  light guide plate fixed colloid color 5.54%, and the  $D$  factor reflector surface difference of 49.25%, in order of importance: difference of reflector surface > color of plastic frame > color of fixed colloid of light guide plate > dot size of light guide plate.

3) The homogeneity has an effect worthy of further research, so that the future backlight module development process can effectively reduce the production cost, improve the efficiency of the production process, and produce the best output by effectively understanding the impact of factors on the uniformity of the backlight module uniform backlight module design.

## Acknowledgements

The authors acknowledge the support by the Ministry of Science and Technology, Taiwan, under grant numbers MOST 109-2221-E-992-009-MY3.

## References

- [1] CHIEN K.-W., SHIEN H.-P.D., *Design and fabrication of an integrated polarized light guide for liquid -crystal-display illumination*, Applied Optics **43**(9), 2004, pp. 1830–1834, DOI: [10.1364/AO.43.001830](https://doi.org/10.1364/AO.43.001830).
- [2] CHANG J.-G., LEE C.-T., FANG Y.-B., HWANG C.-C., *Generation of random non-overlapping dot patterns for light guides using molecular dynamics simulations with variable r-cut and reflective boundary techniques*, Computer Physics Communications **177**(11), 2007, pp. 851–862, DOI: [10.1016/j.cpc.2007.07.010](https://doi.org/10.1016/j.cpc.2007.07.010).

- [3] LIN C.-F., WU C.-C., YANG P.-H., KUO T.-Y., *Application of Taguchi method in light-emitting diode backlight design for wide color gamut displays*, Journal of Display Technology **5**(8), 2009, pp. 323–330, DOI: [10.1109/JDT.2009.2023606](https://doi.org/10.1109/JDT.2009.2023606).
- [4] JOO B.-Y., KANG J.J., HONG J.-P., *Analysis of the light-scattering power of patterned dot material printed on the light guide plate in liquid crystal display*, Displays **33**(4–5), 2012, pp. 178–185, DOI: [10.1016/j.displa.2012.08.005](https://doi.org/10.1016/j.displa.2012.08.005).
- [5] YU J.-C., SUPRAYITNO, YANG L.-W., *Optical design optimization of high contrast light guide plate for front light unit*, Microsystem Technologies **25**(5), 2019, pp. 2135–2144, DOI: [10.1007/s00542-018-04287-x](https://doi.org/10.1007/s00542-018-04287-x).
- [6] ZHENG X., ZHOU S.C., XU R., CHEN H.P., *Energy-efficient scheduling for multi-objective two-stage flow shop using a hybrid ant colony optimisation algorithm*, International Journal of Production Research **58**(13), 2020, pp. 4103–4120, DOI: [10.1080/00207543.2019.1642529](https://doi.org/10.1080/00207543.2019.1642529).
- [7] YEN Y.-T., FANG T.-H., LIN Y.-C., *Optimization of screen-printing parameters of SN9000 ink for pinholes using Taguchi method in chip on film packaging*, Robotics and Computer-Integrated Manufacturing **27**(3), 2011, pp. 531–537, DOI: [10.1016/j.rcim.2010.09.008](https://doi.org/10.1016/j.rcim.2010.09.008).
- [8] KIJASZEK W., OLESZKIEWICZ W., *Optimization of radio frequency inductively coupled plasma enhanced chemical vapour deposition process of diamond-like carbon films*, Optica Applicata **46**(2), 2016, pp. 167–172, DOI: [10.5277/oa160201](https://doi.org/10.5277/oa160201).
- [9] CHEN W.-C., LAI T.-T., WANG M.-W., HUNG H.-W., *An optimization system for LED lens design*, Expert Systems With Applications **38**(9), 2011, pp. 11976–11983, DOI: [10.1016/j.eswa.2011.03.092](https://doi.org/10.1016/j.eswa.2011.03.092).
- [10] LEE S.-C., KIM T., PARK W.-S., *Liquid crystal displays with variable viewing angles using electric field-driven liquid crystal lenses as diffusers*, Applied Sciences **10**(2), 2020, article 667, DOI: [10.3390/app10020667](https://doi.org/10.3390/app10020667).
- [11] TIEN N.X., SHIN S., *A novel concentrator photovoltaic (CPV) system with the improvement of irradiance uniformity and the capturing of diffuse solar radiation*, Applied Sciences **6**(9), 2016, article 251, DOI: [10.3390/app6090251](https://doi.org/10.3390/app6090251).
- [12] HU R., LUO X.B., ZHENG H., QIN Z., GAN Z.Q., WU B.L., LIU S., *Design of a novel freeform lens for LED uniform illumination and conformal phosphor coating*, Optics Express **20**(13), 2012, pp. 13727–13737, DOI: [10.1364/OE.20.013727](https://doi.org/10.1364/OE.20.013727).
- [13] YE Z.T., CHEN C.L., CHEN L.-C., TIEN C.H., NGUYEN H.T., WANG H.-C., *Hollow light guide module involving mini light-emitting diodes for asymmetric luminous planar illuminators*, Energies **12**(14), 2019, article 2755, DOI: [10.3390/en12142755](https://doi.org/10.3390/en12142755).
- [14] HUANG B.-L., GUO T.-L., *Integrated backlight module to provide a collimated and uniform planar light source*, Applied Optics **55**(26), 2016, pp. 7307–7313, DOI: [10.1364/AO.55.007307](https://doi.org/10.1364/AO.55.007307).
- [15] LE H.-T., LE L.-T., LIAO H.-Y., CHEN M.-J., MA H.-Y., LEE H.-Y., *Design of low-glared LED rear light of automotive for EU ECE regulation by use of optimized micro-prisms array*, Crystals **10**(2), 2020, article 63, DOI: [10.3390/cryst10020063](https://doi.org/10.3390/cryst10020063).
- [16] TSAI J.-Z., CHANG R.-S., LI T.-Y., CHUANG T.C., *LED backlight module by a lightguide-diffusive component with tetrahedron reflector array*, Journal of Display Technology **8**(6), 2012, pp. 321–328, DOI: [10.1109/JDT.2012.2184077](https://doi.org/10.1109/JDT.2012.2184077).
- [17] WANG J., SUN S.-F., LIU Q.-Y., SHAO J., ZHANG F.-Y., ZHANG Q., *Effects of laser processing parameters on glass light guide plate scattering dot performance*, Optics & Laser Technology **115**, 2019, pp. 90–96, DOI: [10.1016/j.optlastec.2019.01.033](https://doi.org/10.1016/j.optlastec.2019.01.033).
- [18] KAKINUMA K., *Technology of wide color gamut backlight with light-emitting diode for liquid crystal display television*, Japanese Journal of Applied Physics **45**(5B), 2006, pp. 4330–4334, DOI: [10.1143/JJAP.45.4330](https://doi.org/10.1143/JJAP.45.4330).
- [19] LEE G., JEONG J.H., YOON S.-J., CHOI D.-H., *Design optimization for optical patterns in a light-guide panel to improve illuminance and uniformity of the liquid-crystal display*, Optical Engineering **48**(2), 2009, article 024001, DOI: [10.1117/1.3083290](https://doi.org/10.1117/1.3083290).

- [20] KIM G.H., KIM W.J., KIM S.M., SON J.G., *Analysis of thermo-physical and optical properties of a diffuser using PET/PC/PBT copolymer in LCD backlight units*, *Displays* **26**(1), 2005, pp. 37–43, DOI: [10.1016/j.displa.2004.11.001](https://doi.org/10.1016/j.displa.2004.11.001).
- [21] YANG X.P., YAN Y.B., FENG D., JIN G.F., *Compound hyperbolic concentrator-type reflectors for liquid crystal display backlight systems*, *Journal of Optics A: Pure and Applied Optics* **7**(9), 2005, pp. 514–518, DOI: [10.1088/1464-4258/7/9/011](https://doi.org/10.1088/1464-4258/7/9/011).

*Received September 9, 2020  
in revised form January 12, 2021*